INTERNATIONAL JOURNAL FOR NUMERICAL METHODS IN FLUIDS
Int. J. Numer. Meth. Fluids 2001; **35**: 575–591

The two-dimensional streamline upwind scheme for the convection–reaction equation

Tony W. H. Sheu*,[1] and H. Y. Shiah

Department of Naval Architecture and Ocean Engineering, National Taiwan University, Taipei, Taiwan

SUMMARY

This paper is concerned with the development of the finite element method in simulating scalar transport, governed by the convection–reaction (CR) equation. A feature of the proposed finite element model is its ability to provide nodally exact solutions in the one-dimensional case. Details of the derivation of the upwind scheme on quadratic elements are given. Extension of the one-dimensional nodally exact scheme to the two-dimensional model equation involves the use of a streamline upwind operator. As the modified equations show in the four types of element, physically relevant discretization error terms are added to the flow direction and help stabilize the discrete system. The proposed method is referred to as the streamline upwind Petrov–Galerkin finite element model. This model has been validated against test problems that are amenable to analytical solutions. In addition to a fundamental study of the scheme, numerical results that demonstrate the validity of the method are presented. Copyright © 2001 John Wiley & Sons, Ltd.

KEY WORDS: convection–reaction equation; nodally exact; Petrov–Galerkin; streamline upwind; two-dimensional

1. INTRODUCTION

There exist many flow situations in which reaction terms are present, and modeling of them is important. Typical examples in engineering are the Helmholtz equations for modeling sound propagation [1], κ–ϵ equations for modeling flow turbulence [2], and constitutive equations for modeling extra stresses in non-Newtonian flow motion [3]. In this paper, we are concerned with equations for the viscoelastic fluid flow. The prototype equation for this class of flow is the convection–reaction (CR) equation. Methods of solving transport equations containing reaction terms are mostly constructed from physically more complex convection–diffusion–reaction (CDR) equations [4–7]. Very few if any have been directly developed from the CR

* Correspondence to: Department of Naval Architecture and Ocean Engineering, National Taiwan University, 73 Chou-Shan Road, Taipei, Taiwan. Tel.: + 886 2 23625470, ext. 246; fax: + 886 2 23929885.
[1] E-mail: tony.sheu@cfd.na.ntu.edu.tw

Received April 1999
Revised May 2000

equation. At first glance it appears that one might directly apply the CDR models by setting the diffusion coefficient to zero [5–7]. A problem that occurs in the use of CDR discrete models is that of the zero denominator in the scheme coefficients, which make the application of CDR models impractical. In this light, it is legitimate to deal with modeling the CR equation directly and this motivates the present study.

A reliable simulation model requires a numerical scheme that has the ability to predict transport phenomena accurately while being able to suppress numerical instability that arises in the course of discretization. The problem with numerical instability is important since advective and reactive terms can cause the solutions to diverge. It is then a question of constructing proper upwind schemes that can stabilize the finite element equation. From the stability viewpoint, it is computationally more difficult to solve transport equations with vanishing fluid viscosity. Due to the absence of physical damping terms, which aid stabilization of the discrete system, care must be taken in the approximation of direction-dependent advection terms to avoid convective instability. This is particularly the case in multi-dimensional analyses. In this paper we are also concerned with prediction accuracy, since we do not regard a scheme as useful if it cannot provide a high level of accuracy. In addition, a lack of alignment of co-ordinate lines with flow directions can cause the prediction accuracy to deteriorate in the computation for two-dimensional flow problems [8]. Another aim of the present paper is to elucidate a means of resolving this problem.

The rest of this paper is organized as follows. In Section 2 the finite element model is first presented based on the one-dimensional case in order to provide an analytical representation of the solution. This is followed by extending the scheme to multi-dimensional analysis, with an emphasis on the choice of the weighting function. The streamline upwind operator is introduced into the formulation to add a stabilizing term along the flow direction. Section 3 is devoted to explaining why the working equation is worth considering. Section 4 gives numerical results that demonstrate the validity of this method. In Section 5 we make concluding remarks.

2. FINITE ELEMENT ANALYSIS OF THE CONVECTION–REACTION EQUATION

Each constitutive equation governing transport of an extra-stress component ϕ in non-Newtonian fluid flows is as follows:

$$u\frac{\partial \phi}{\partial x} + v\frac{\partial \phi}{\partial y} + c\phi = f \tag{1}$$

In the above, c is the coefficient of the reaction term and f denotes the source term. To a first approximation, velocity components u and v are considered as constant values. In this paper, we are concerned with the development of the finite element model that can provide good stability and high accuracy for Equation (1). The underlying idea is that the scheme presented here provides nodally exact solutions for the one-dimensional case. As the dimension increases by one, artificial viscosity needed to stabilize the discrete system is added along the flow direction to avoid false diffusion errors [9].

2.1. One-dimensional convection–reaction finite element model

As already mentioned, we consider first the finite element analysis of the following one-dimensional model equation:

$$u\frac{\partial \phi}{\partial x} + c\phi = f \tag{2}$$

To solve the above equation, the Petrov–Galerkin finite element model is developed in a domain that is covered with uniform quadratic elements. As is the case when conducting weighted residuals finite element analysis, the basis space $\{N_i\}$ for the field variable ϕ and the test space $\{W_i\}$ for Equation (2) need to be defined. Figure 1 shows two quadratic finite elements, each of which has a grid size of $2h$. For stability reasons, the discrete model must be constructed within the Petrov–Galerkin finite element framework. As with the development of the CR finite element model [8], it is required that $\alpha h N_i'$ be added to N_i, thus obtaining the weighting function

$$W_i = N_i + \alpha h N_i' \tag{3}$$

The introduced free parameter α determines the weight placed in favor of the upwind side node.

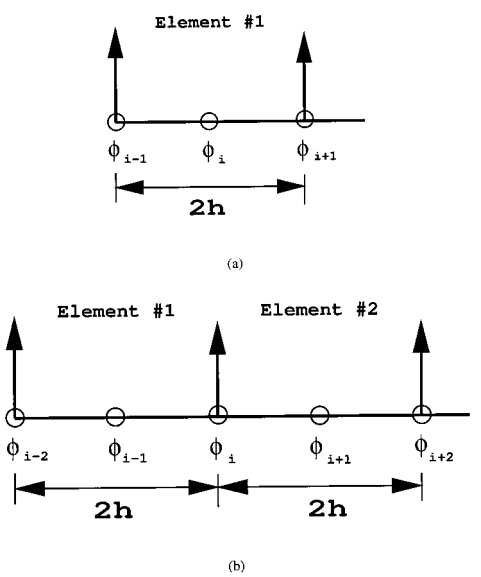

Figure 1. An illustration of an one-dimensional quadratic element with the uniform grid size $2h$. (a) middle node representation; (b) corner node representation.

The derivation is followed by substituting the quadratic shape function $(N_1, N_2, N_3) = ((\xi-1)\xi/2, (1+\xi)(1-\xi), (1+\xi)\xi/2)$ and the weighting function given in Equation (3) into the weighting residuals statement

$$\sum_e \int_{\Omega_e} W_i\left(u\frac{\partial\phi}{\partial x} + c\phi - f\right) \mathrm{d}x = 0 \tag{4}$$

In the above, ξ $(-1 \le \xi \le 1)$ denotes the co-ordinate for the master element. After some algebra, the discrete equations similar to the finite difference equations are derived. Since the quadratic element, shown schematically in Figure 1, is used, discrete equations are presented at the middle and corner nodes respectively. Due to space limitations we will omit the detailed derivation of the discrete equations but rather summarize them as below

Middle node i shown in Figure 1(a)

$$\frac{u}{h}\left(\left(-\frac{2}{3}-\frac{4\alpha}{3}\right)\phi_{i-1} + \frac{8\alpha}{3}\phi_i + \left(\frac{2}{3}-\frac{4\alpha}{3}\right)\phi_{i+1}\right) + c\left(\left(\frac{2}{15}+\frac{2\alpha}{3}\right)\phi_{i-1} + \frac{16}{15}\phi_i + \left(\frac{2}{15}-\frac{2\alpha}{3}\right)\phi_{i+1}\right) = \frac{4}{3}f \tag{5}$$

Corner node i shown in Figure 1(b)

$$\frac{u}{h}\left(\left(\frac{1}{6}+\frac{\alpha}{6}\right)\phi_{i-2} + \left(-\frac{2}{3}-\frac{4\alpha}{3}\right)\phi_{i-1} + \frac{14\alpha}{6}\phi_i + \left(\frac{2}{3}-\frac{4\alpha}{3}\right)\phi_{i+1} + \left(-\frac{1}{6}+\frac{\alpha}{6}\right)\phi_{i+2}\right) + c\left(\left(-\frac{1}{15}-\frac{\alpha}{6}\right)\phi_{i-2} + \left(\frac{2}{15}+\frac{2\alpha}{3}\right)\phi_{i-1} + \frac{8}{15}\phi_i + \left(\frac{2}{15}-\frac{2\alpha}{3}\right)\phi_{i+1} + \left(-\frac{1}{15}+\frac{\alpha}{6}\right)\phi_{i+2}\right) = \frac{2}{3}f \tag{6}$$

Although the derivation of the above algebraic equations is quite involved, Equations (5) and (6) are useful in the determination of the value of α, by means of which more accurate solutions can be obtained using the weighted residuals method.

Having obtained the local representation of the Petrov–Galerkin finite element equation, we need to determine the free parameter α so that the solutions obtained can be nodally exact. To achieve this goal, the following analytical solution for Equation (2) is taken into consideration:

$$\phi = C\,\mathrm{e}^{-cx/u} + \frac{f}{c} \tag{7}$$

In the above C is a constant. By making use of this analytical representation of ϕ, one can obtain the exact expressions for ϕ_{i-2}, ϕ_{i-1}, ϕ_i, ϕ_{i+1}, and ϕ_{i+2}. The derivation of the analytical α is followed by substitution of these analytical values into Equations (5) and (6), from which the analytical expressions of α at the middle and corner nodes can be derived. By defining the dimensionless parameter β as

$$\beta = \frac{ch}{u} \tag{8}$$

the analytical α can be obtained as

$$\alpha_{\text{middle node}} = \frac{4\beta + \beta\cosh(\beta) - 5\sinh(\beta)}{5(2\cosh(\beta) - \beta\sinh(\beta) - 2)} \tag{9}$$

$$\alpha_{\text{corner node}} = \frac{8\beta + 4\beta\cosh(\beta) - 2\beta\cosh(2\beta) - 20\sinh(\beta) + 5\sinh(2\beta)}{5(8\cosh(\beta) - \cosh(2\beta) - 4\beta\sinh(\beta) + \beta\sinh(2\beta) - 7)} \tag{10}$$

As Figures 2 and 3 show, the analytical values of α given in Equations (9) and (10) approach their asymptotic values, -0.1975 and -0.3975 respectively, as $|\beta|$ continuously increases.

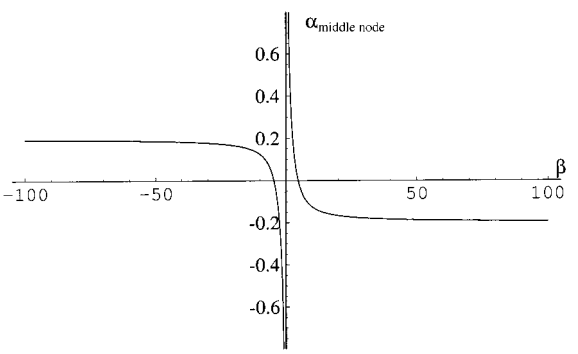

Figure 2. The analytical expression of α, shown in Equation (9), against $\beta = ch/u$ at the middle node.

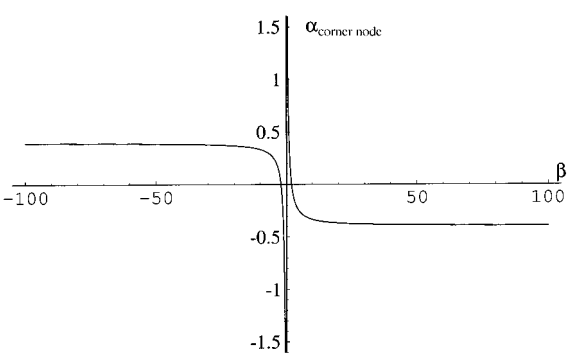

Figure 3. The analytical expression of α, shown in Equation (10), against $\beta = ch/u$ at the corner node.

2.2. Streamline upwind convection–reaction finite element model

Having derived the analytical one-dimensional Petrov–Galerkin finite element model for Equation (2), we now proceed to extend the analysis scope. Within the two-dimensional context it is desired that this scheme is computationally stable and numerically accurate. For this reason one can employ the strategy of adding stabilizing terms mainly along the primary flow direction. Following the idea of Hughes and Brooks [8], the weighting functions employed in this paper for solving Equation (1) are as follows:

$$W_i = N_i + \tau\left(u\frac{\partial N_i}{\partial x} + v\frac{\partial N_i}{\partial y}\right) \tag{11}$$

or

$$W_i = N_i + \tau_i \frac{N^j \tilde{V}_k^j}{\sqrt{u^2+v^2}}\frac{\partial N_i}{\partial x_k} \tag{12}$$

where

$$\tau_i = \frac{\sum_{i=1}^{n} \delta(\gamma_{Y_i}) V_{Y_i} h_{Y_i}}{2\sqrt{u^2+v^2}} \tag{13}$$

The finite element formulation is followed by substitution of weighting and shape functions into the weighted residuals statements for Equation (1) to derive the algebraic equations. Since bi-quadratic elements are considered, discrete equations should be obtained for the four element types shown schematically in Figure 4. The derivation of these discrete equations is quite a delicate task. After some algebra, the modified Equation (1) can be derived. Depending on the element types, these modified equations are summarized in the following:

$$u\phi_x + v\phi_y + c\phi - f = \tau\{uc\phi_x + vc\phi_y + u^2\phi_{xx} + v^2\phi_{yy} + 2uv\phi_{xy}\} + S' \tag{14}$$

The error terms S' in Equation (14) are shown in Table I for the reader's reference.

Equation (14) has novel features worth noting. Taking the second derivative of ϕ along the flow direction, s, into consideration, we can obtain the following identity equation in the physical co-ordinate system (x, y):

$$\phi_{ss} = \frac{u^2}{u^2+v^2}\frac{\partial^2\phi}{\partial x^2} + \frac{2uv}{u^2+v^2}\frac{\partial^2\phi}{\partial x\,\partial y} + \frac{v^2}{u^2+v^2}\frac{\partial^2\phi}{\partial y^2} \tag{15}$$

According to Equations (14) and (15), the leading dissipative discretization error is added mainly along the flow direction θ ($\equiv \tan^{-1}(v/u)$). This derivation explains why the above weighted residuals statement is referred to as being a streamline upwind Petrov–Galerkin (SUPG) finite element model. Owing to the introduction of ϕ_{ss} into the finite element

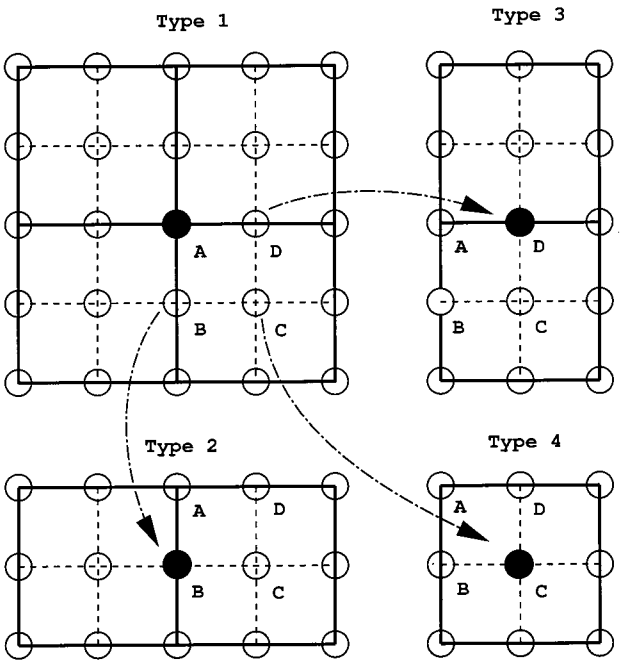

Figure 4. Four types of element encountered in the bi-quadratic elements.

formulation, it clarifies the rationale of applying the weighting function given in Equation (12) to stabilize the scheme. In summary, the leading discretization error is added along the streamline and helps stabilize the discrete system with no cross-wind diffusion.

3. APPLICATION TO VISCOELASTIC PROBLEMS

We will next apply the developed CR finite element model together with the streamline finite element model [10] to simulate the incompressible Navier–Stokes equations. Under the assumption that the fluid density, ρ, is constant, a non-Newtonian fluid flow will be considered in a domain of two dimensions. Neglecting the effect of gravity and taking the flow as being steady, the flow can be described by the continuity equation and the Navier–Stokes equations given below respectively

$$\nabla \cdot \underline{u} = 0 \tag{16}$$

$$\rho \underline{u} \cdot \nabla \underline{u} = -\nabla p + \nabla \underline{\underline{T}} \tag{17}$$

In the above, the extra-stress tensor $\underline{\underline{T}}$ ($\equiv T_{ij}$) is defined as follows:

Table I. Discretization error terms derived for four types of elements using the quadratic upwind finite element model.

Element type	Discretization error terms S'
Type 1	$h^2\left[\frac{c}{5}(\phi_{xx}+\phi_{yy})+\frac{u}{30}(10T_{xxx}+6\phi_{xyy})+\frac{v}{30}(6\phi_{xxy}+10\phi_{yyy})\right]$ $+\frac{\tau c}{15}(-5u\phi_{xxx}-5v\phi_{yyy}-3v\phi_{xxy}-3u\phi_{xyy})$
Type 2	$h^2\left[\frac{c}{10}(2\phi_{xx}-\phi_{yy})+\frac{u}{30}(10\phi_{xxx}-3\phi_{xyy})+\frac{v}{30}(6\phi_{xxy}-5\phi_{yyy})\right]$ $+\frac{\tau c}{30}(5v\phi_{yyy}-10u\phi_{xxx}+3u\phi_{xyy}-6u\phi_{xxy})$
Type 3	$h^2\left[\frac{c}{10}(-\phi_{xx}+2\phi_{yy})+\frac{u}{30}(-5\phi_{xxx}+6\phi_{xyy})-\frac{v}{30}(3\phi_{xxy}-10\phi_{yyy})\right]$ $+\frac{\tau c}{30}(5u\phi_{xxx}-10v\phi_{yyy}+3v\phi_{xxy}-6v\phi_{xyy})$
Type 4	$h^2\left[\frac{c}{10}(-\phi_{xx}-\phi_{yy})+\frac{u}{30}(-5\phi_{xxx}-3\phi_{xyy})-\frac{v}{30}(3\phi_{xxy}+5\phi_{yyy})\right]$ $+\frac{\tau c}{30}(5u\phi_{xxx}+5v\phi_{yyy}+3v\phi_{xxy}+3u\phi_{xyy})$

$$T_{ij}=2\bar{\mu}D_{ij} \tag{18}$$

where

$$D_{ij}=\frac{1}{2}\left(\frac{\partial u_i}{\partial x_j}+\frac{\partial u_j}{\partial x_i}\right)$$

denotes the rate of deformation tensor. The coefficient $\bar{\mu}$ in Equation (18) is called the apparent viscosity. Unlike the Newtonian fluid flow, where $\bar{\mu}$ is a constant value, the apparent viscosity depends on D_{ij} to account for the elastic nature embedded in the fluid flow.

When solving Equations (16) and (17) together with appropriate boundary conditions, the difficulty is the determination of constitutive equations for T_{ij}. Of two major classes of constitutive equations, the differential equation model has gained wider popularity in simulation since it is easier to be solved simultaneously with the differential equations (16) and (17). Among the constitutive equations for T_{ij} found in the open literature, the general Oldroyd differential model has been regarded as being general [3]. One aim of the present paper is to apply the new finite element model just described to solve constitutive equations for T_{ij}. A variant of the general Oldroyd model, called Oldroyd-B constitutive equation, will be considered in this paper as an example. The equation given below for this fluid is adequate to describe the rheology of some polymer solutions [3]

$$\underline{\underline{T}} + \lambda_1 \overset{\nabla}{\underline{\underline{T}}} = 2\mu\left(\underline{\underline{D}} + \lambda_2 \overset{\nabla}{\underline{\underline{D}}}\right) \tag{19}$$

where μ is the shear viscosity. In Equation (19), λ_1 and λ_2 denote the relaxation time and the retardation time respectively.

In this analysis, $\underline{\underline{T}}$ is decomposed into two parts, namely $\underline{\underline{T_1}}$ and $\underline{\underline{T_2}}$. With $\underline{\underline{T}} = \underline{\underline{T_1}} + \underline{\underline{T_2}}$, Equation (19) can be easily shown to be identical to the following two equations:

$$\underline{\underline{T_1}} + \lambda_1 \overset{\nabla}{\underline{\underline{T_1}}} = 2\mu_1 \underline{\underline{D}} \tag{20}$$

$$\underline{\underline{T_2}} = 2\mu_2 \underline{\underline{D}} \tag{21}$$

In the above, $\overset{\nabla}{\underline{\underline{T}}}$ represents the upper-convective of $\underline{\underline{T}}$

$$\overset{\nabla}{\underline{\underline{T}}} = \frac{\mathrm{D}\underline{\underline{T}}}{\mathrm{D}t} - (\nabla \underline{u})^T \cdot \underline{\underline{T}} - \underline{\underline{T}} \cdot \nabla \underline{u} \tag{22}$$

Equations (20)–(22) are derived under the conditions that $\mu = \mu_1 + \mu_2$ and $\lambda_2/\lambda_1 = \mu_2/\mu_1$. Examining of $\underline{\underline{T_2}}$ from Equation (17) we obtain the following working equations, which can be used together with the continuity equation (16), for the Oldroyd-B non-Newtonian fluid flow simulation [4]:

$$\underline{\underline{T_1}} + \lambda_1 \overset{\nabla}{\underline{\underline{T_1}}} = 2\mu_1 \underline{\underline{D}} \tag{23}$$

$$\rho(\underline{u} \cdot \nabla)\underline{u} = -\nabla p + 2\mu_2 \nabla \cdot \underline{\underline{D}} + \nabla \cdot \underline{\underline{T_1}} \tag{24}$$

A comparison of the working equations for the Newtonian fluid and its non-Newtonian counterpart reveals the necessity of developing an accurate finite element model for analyzing Equation (23). This opens up a way to extend the flow models into many different areas.

The equation employed in the simulation is the dimensionless form of Equation (23). The resulting dimensionless equation has the same form as Equation (23) except for the introduction of the Weissenberg number, *We*, into the formulation

$$\underline{\underline{T}}^* + We \overset{\nabla}{\underline{\underline{T_1}}}^* = 2\underline{\underline{D}}^* \tag{25}$$

In the above, the Weissenberg number obtained in the normalization procedure is

$$We = \frac{\lambda_1 u_{\mathrm{ref}}}{l_{\mathrm{ref}}} \tag{26}$$

where u_{ref} and l_{ref} denote the reference velocity and length respectively. In what follows, the superscript * is omitted for simplicity. Substituting Equation (22) for $\overset{\nabla}{\underline{\underline{T_1}}}$, Equation (25) can be expressed explicitly as follows:

Table II. Expressions of c_ϕ and S_ϕ, shown in Equation (27), for different stress components.

ϕ	c_ϕ	S_ϕ
T_{11}	$1-2We\dfrac{\partial u}{\partial x}$	$2\dfrac{\partial u}{\partial x}+We\left[\dfrac{\partial u}{\partial y}T_{12}+\dfrac{\partial u}{\partial y}T_{21}\right]$
T_{12}	$1-2We\left(\dfrac{\partial u}{\partial x}+\dfrac{\partial v}{\partial y}\right)$	$\dfrac{\partial u}{\partial y}+\dfrac{\partial v}{\partial x}+We\left[\dfrac{\partial u}{\partial y}T_{22}+\dfrac{\partial v}{\partial x}T_{11}\right]$
T_{22}	$1-2We\dfrac{\partial v}{\partial y}$	$2\dfrac{\partial v}{\partial y}+We\left[\dfrac{\partial v}{\partial x}T_{12}+\dfrac{\partial v}{\partial x}T_{21}\right]$

$$\bar{u}\frac{\partial \phi}{\partial x}+\bar{v}\frac{\partial \phi}{\partial y}+c_\phi\phi=S_\phi \tag{27}$$

where $\bar{u}=uWe$, $\bar{v}=vWe$, and S_ϕ are tabulated in Table II.

4. NUMERICAL RESULTS

4.1. Benchmark tests

As is the case whenever a new scheme for solving a different equation is presented, the finite element model presented in Section 2 needs to be validated. For this reason, we resort to test problems that are amenable to analytical solutions. For a first approximation, coefficients u and c in Equation (2) are assumed to be constant values: $u=1$ and $c=100$. Under the assumption that $f=1$, the analytical solution for the model equation is derived as

$$\phi=\frac{1}{100}+\mathrm{e}^{-100x} \tag{28}$$

In this calculation, uniform mesh points are overlaid in the physical domain $0\leq x\leq 1$. The computed result, shown in Figure 5, is seen to reproduce the analytical solution to the test equation. This test proves that the proposed finite element model can provide a nodally exact solution for the CR model equation.

Having validated the code through the one-dimensional test problem, we will now examine the degree of deterioration of the predication accuracy when two-dimensional problems are considered. To assess the accuracy and allow comparison with analytical solutions, the test problem chosen in this paper involves constant values of u, v, and c in the domain $0\leq x, y\leq 1$

$$\frac{1}{\sqrt{2}}\left(\frac{\partial \phi}{\partial x}+\frac{\partial \phi}{\partial y}\right)+\phi=1 \tag{29}$$

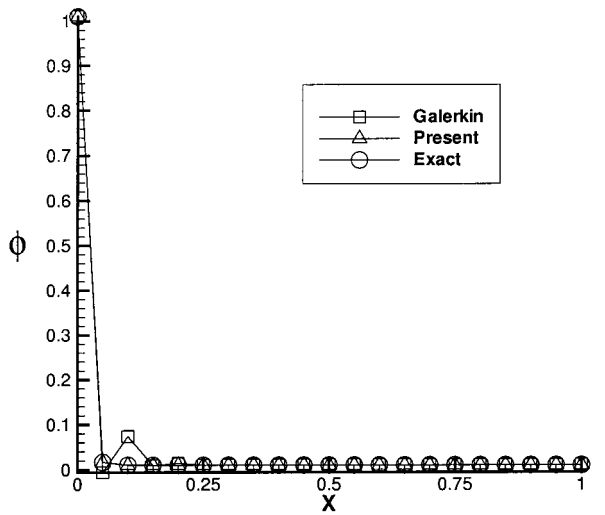

Figure 5. A comparison of the computed and exact solutions shown in Equation (28).

The above equation, subject to boundary conditions schematically shown in Figure 6, is amenable to the following exact solution:

$$\phi = 1 + \mathrm{e}^{-(x+y)/\sqrt{2}} \tag{30}$$

The region of interest was overlaid with uniform girds. The computed results indicate that good agreement has been obtained with exact solutions, thus demonstrating the integrity of the method. To further obtain the rate of convergence that this scheme can provide, computations

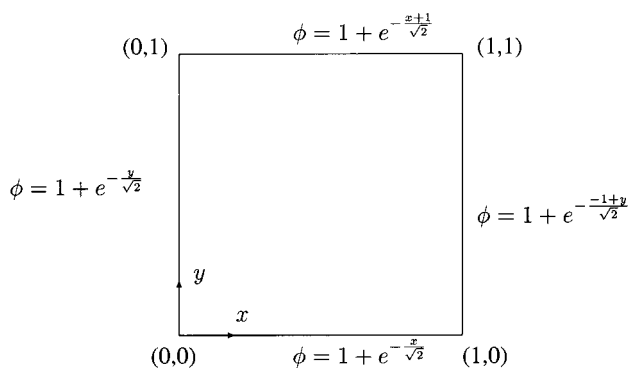

Figure 6. An illustration of the boundary conditions for the test problem.

were performed on increasingly refined uniform grids. Results thus obtained were cast in their L_2-error norms and plotted against grid-size ratios. As Figure 7 shows, the rate of convergence of the proposed SUPG CR finite element model is 1.42.

The check of the integrity of the finite element model was followed by considering a more stringent problem. In a square domain of unit length, the constant flow had a magnitude of 1 and an angle of $\theta = \tan^{-1}(v/u) = 45°$. This problem was considered in order to assess whether the proposed finite element model could capture sharp changes in field variables in the flow interior. Considered the model problem given by

$$\frac{1}{\sqrt{2}}\left(\frac{\partial \phi}{\partial x} + \frac{\partial \phi}{\partial y}\right) + \phi = 0 \tag{31a}$$

$$\phi(x = 0, y) = 1 + \mathrm{e}^{-(x+y)/\sqrt{2}} \tag{31b}$$

$$\phi(x = 1, y) = 1 \tag{31c}$$

$$\phi(x, y = 0) = 1 \tag{31d}$$

$$\phi(x, y = 1) = 1 + \mathrm{e}^{-(x+y)/\sqrt{2}} \tag{31e}$$

The solutions were computed in the domain covered with uniform grids with $\Delta x = \Delta y = 0.025$. The computed contours of ϕ are shown in Figure 8. For the sake of clarity, the sectional profiles of the computed ϕ are also plotted. Revealed by Figure 9 is a drastic change of ϕ across the line $x - y = 0$. This demonstrates the utility of the CR scheme in capturing high-gradient solutions. For comparison purposes, we also plot Galerkin solutions in Figure 9 to show that oscillations have been well suppressed by the proposed streamline upwind model.

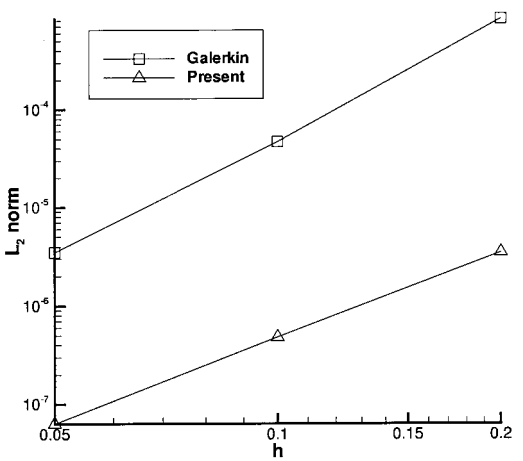

Figure 7. The plot of L_2-error norms against the grid spacings for showing the rate of convergence.

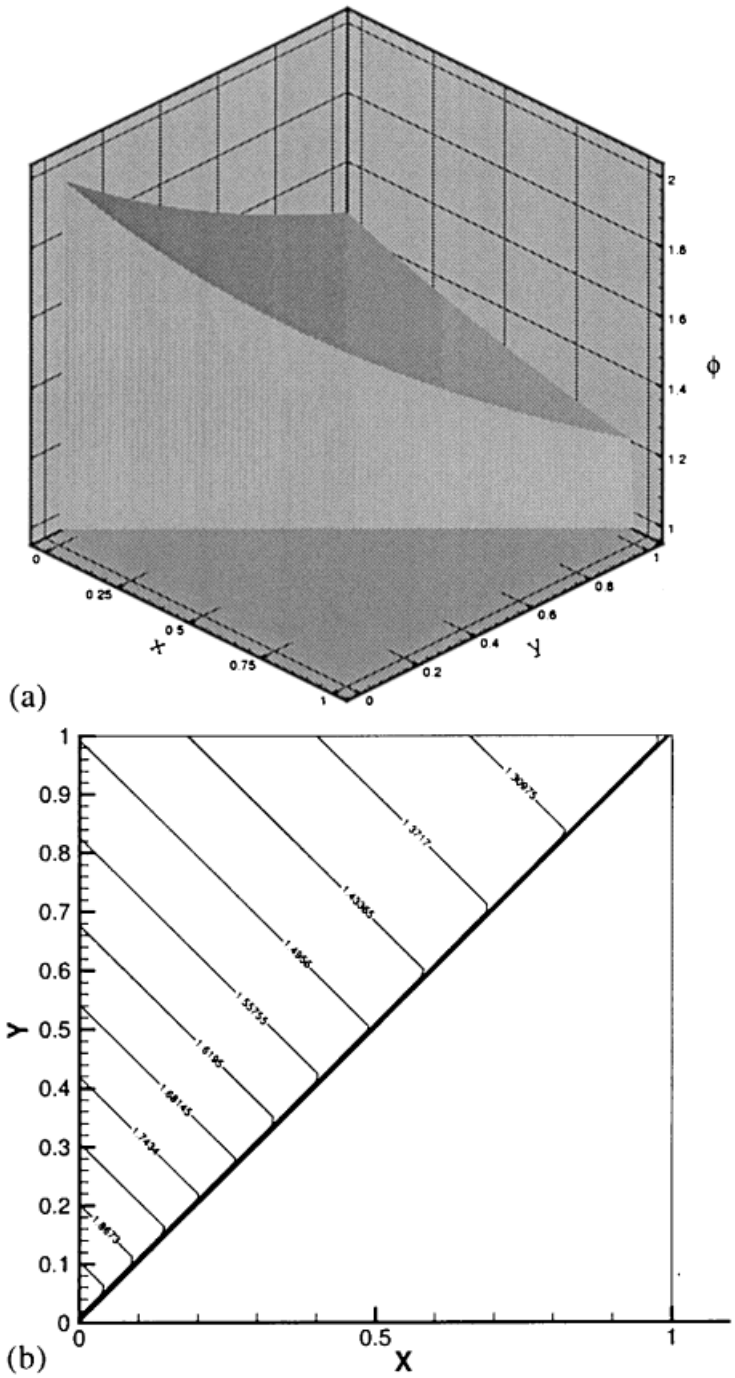

Figure 8. The computed contour values of ϕ. (a) Three-dimensional plot of ϕ; (b) contour plots of ϕ.

4.2. Plane Poiseuille non-Newtonian flow problem

As a validation study, we consider a simple problem that has an analytical solution. The most-simple case of a non-Newtonian test problem is the plane Poiseuille problem. Given a fully developed velocity profile $(u, v) = (y - y^2, 0)$, the equations governing the non-Newtonian

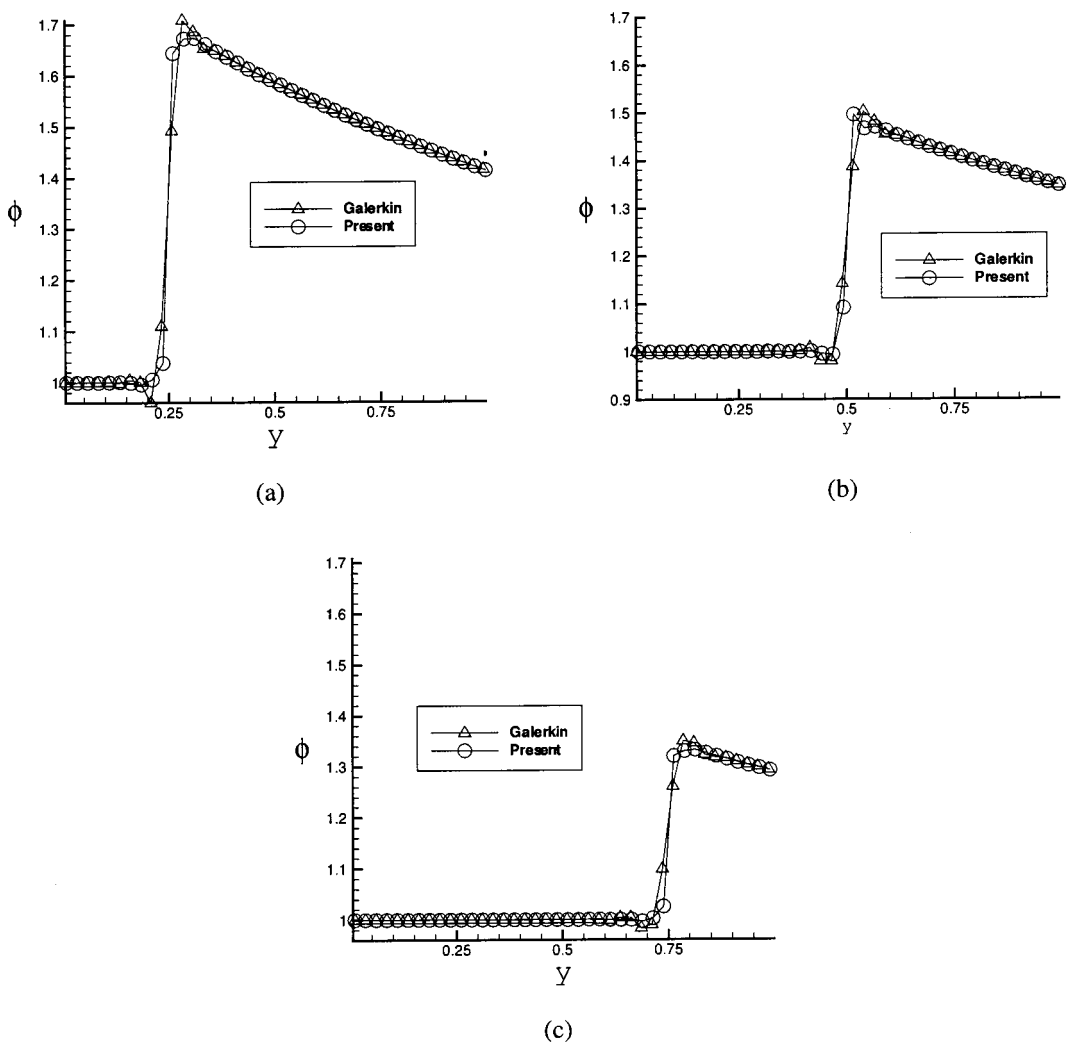

Figure 9. Distributions of ϕ at (a) $x = 0.25$; (b) $x = 0.5$; (c) $x = 0.75$ for the present and Galerkin solutions.

flow motion in the domain shown in Figure 10 are as follows:

$$-\frac{\partial p}{\partial x}+\frac{1}{Re_1}\frac{\partial^2 u}{\partial y^2}+\frac{1}{Re_2}\frac{\partial T_{12}}{\partial y}=0 \tag{32}$$

$$-\frac{\partial p}{\partial y}+\frac{1}{Re_2}\frac{\partial T_{22}}{\partial y}=0 \tag{33}$$

$$T_{11}-2We\frac{\partial u}{\partial y}T_{12}=0 \tag{34}$$

$$T_{12}-We\frac{\partial u}{\partial y}T_{22}=\frac{\partial u}{\partial y} \tag{35}$$

$$T_{22}=0 \tag{36}$$

The extra-stress components can be exactly obtained as follows provided that the boundary conditions are prescribed as those shown in Figure 11:

$$T_{11}=2We(1-2y)^2 \tag{37}$$

$$T_{12}=(1-2y) \tag{38}$$

$$T_{22}=0 \tag{39}$$

The calculation was done for the case of $Re=0.1$ in the uniform mesh overlaid in $0\le x$, $y\le 1$. Three Weissenberg numbers, $We=1$, 10, and 100, were investigated. The results shown in Figure 11 reveal exact agreement with analytical solutions. Also revealed in these figures is that both velocity u and pressure p are invariant with We. This study has demonstrated the

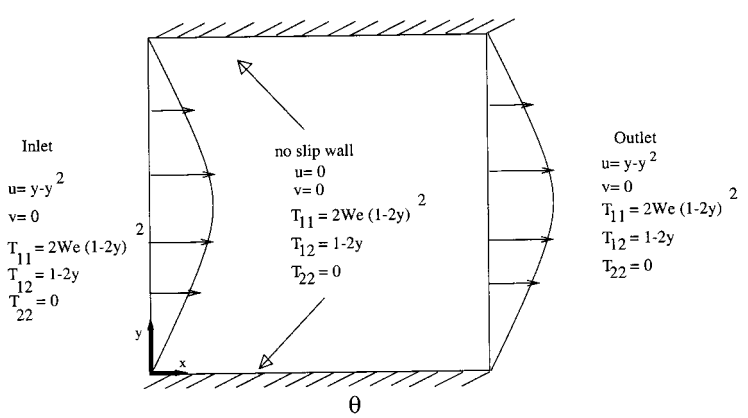

Figure 10. A schematic of the plane Poiseuille test problem and the associated boundary conditions.

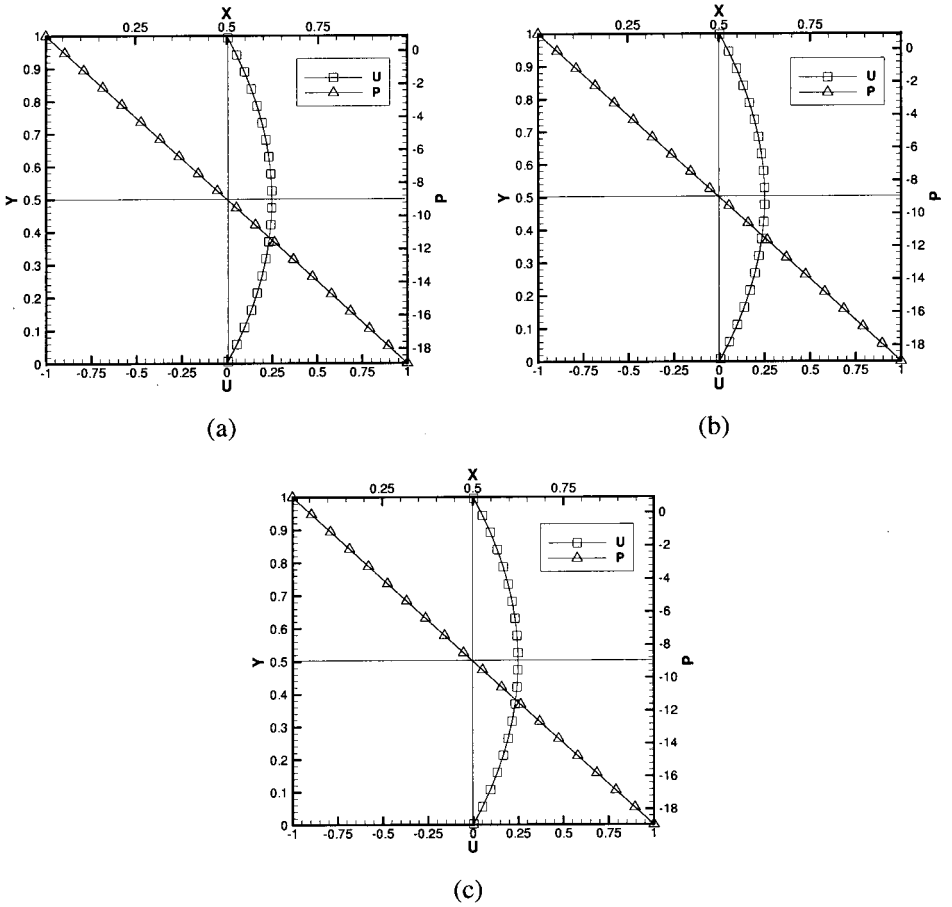

Figure 11. The computed u ($x = 0.5$, y) and p (x, $y = 0.5$) for the plane Poiseuille flow calculated at $Re = 0.1$. (a) $We = 1.0$; (b) $We = 10$; (c) $We = 100$.

applicability of the CR scheme, when used together with the Navier–Stokes flow calculation, to simulate non-Newtonian fluid flow.

5. CONCLUDING REMARKS

In this paper, a finite element model for solving the CR transport equation in quadratic elements is presented. For the sake of accuracy, we have made use of the analytical solution in the course of finite element formulation. Depending on the nodal classification, optimal amounts of upwinding derived in this paper yield a nodally exact one-dimensional upwind

finite element model. To avoid deterioration of the solution due to false diffusion errors in two-dimensional analysis, the streamline upwind operator is developed and is used together with the analytical upwinding coefficients, developed on a one-dimensional basis. This helps add an artificial damping term along the flow direction. Good agreement has been obtained with exact solutions, thus demonstrating the accuracy of the method. In addition, a fundamental study of the method has also been conducted to shed further light on the nature of the scheme has also been applied to simulate the transport equation for extra stresses involved in the equations of motion for viscoelastic flow problems. The results obtained are in perfect agreement with the exact solutions, demonstrating the integrity of the proposed method.

ACKNOWLEDGMENTS

The research support in this work was financially supported by grant NSC88-2611-E-002-025 of Republic of China.

REFERENCES

1. Babuška I, Ihlenburg F, Paik ET, Sauter SA. A generalized finite element method for solving the Helmholtz equation in two dimensions with minimal pollution. *Computer Methods in Applied Mechanics and Engineering* 1995; **128**: 325–359.
2. Ilinca F, Pelletier D. Positivity preservation and adaptive solution for the k–ϵ model of turbulence. *AIAA Journal* 1998; **36**(1): 44–50.
3. Crochet MJ, Davies AR, Walters K. *Numerical Simulation of Non-Newtonian Flow*, *Rheology Series 1*. Elsevier: New York, 1984.
4. Tezduyar T, Park Y. Discontinuity capturing finite element formulations for non-linear convection–diffusion–reaction equations. *Computer Methods in Applied Mechanics and Engineering* 1986; **59**: 307–325.
5. Harari I, Hughes TJR. Stabilized finite element methods for steady advection–diffusion with production. *Computer Methods in Applied Mechanics and Engineering* 1994; **115**: 165–191.
6. Idelsohn S, Nigro N, Storti M, Buscaglia G. A Petrov–Galerkin formulation for advection–reaction–diffusion problems. *Computer Methods in Applied Mechanics and Engineering* 1996; **136**: 27–46.
7. Codina R. Comparison of some finite element methods for solving the diffusion–convection–reaction equation. *Computer Methods in Applied Mechanics and Engineering* 1998; **156**: 185–210.
8. Hughes TJR, Brooks A. A multi-dimensional upwind scheme with no cross wind diffusion. In *Finite Elements for Convection Dominated Flows*, Hughes TJR (ed.). AMD 34, ASME: Washington, DC, 1979.
9. Raithby GD. A critical evaluation of upstream differencing applied to problems involving fluid flow. *Computer Methods in Applied Mechanics and Engineering* 1976; **9**: 75–103.
10. Sheu TWH, Tsai SF, Wang MMT. A Petrov–Galerkin formulation for incompressible flow at high Reynolds number. *Computational Fluid Dynamics* 1995; **5**: 213–230.

